Cross sections for ionization of gases by 10—2000-keV He^+ ions and for electron capture and loss by 5—350-keV He^+ ions

M. E. Rudd, T. V. Goffe,* and A. Itoh
University of Nebraska—Lincoln, Behlen Laboratory of Physics, Lincoln, Nebraska 68588-0111

R. D. DuBois
Pacific Northwest Laboratory, Battelle Memorial Institute, Richland, Washington 99352
(Received 4 February 1985)

Cross sections for production of positive and negative charge for 10—2000-keV He^+ ions on He, Ne, Ar, Kr, H_2, N_2, CO, O_2, CH_4, and CO_2 were measured by the transverse-field method. Electron-capture and -loss cross sections for 5—350-keV He^+ ions on the same targets were measured by the method of beam deflection of various charge states after passing through a known length of target gas. Secondary-emission detectors were used to detect neutral, singly charged, and doubly charged beam components. The equation $\sigma_+ - \sigma_- = \sigma_{10} - \sigma_{12}$ relating the four measured cross sections was utilized to make a least-squares adjustment of the data.

I. INTRODUCTION

There are only three basic inelastic processes that can take place when an energetic ion makes a collision with a neutral atom. These are ejection of electrons from the target or the projectile, transfer of electrons between target and projectile, and excitation of either collision partner. Measurements of the first two of these are described in this paper. Because of their fundamental nature, a knowledge of the cross sections for these processes is essential in many applied areas, but theoretical methods to deal with projectiles carrying one or more electrons are not yet well developed.

The quantities measured are σ_+, the cross section for production of slow positive charge, σ_-, the cross section for production of slow negative charge, σ_{10}, the capture cross section, and σ_{12} the loss cross section.

While numerous measurements are available for some of these cross sections for specific targets, a survey of the literature reveals many gaps and inconsistencies. In the reports on ionization,[1–5] there is little data on CO and none at all on CO_2 or CH_4. Among the N_2 data there are 20—45 % discrepancies. The small amount of data for O_2 disagree by 65% where they overlap. While there is abundant data for most of the rare gases, even here there are 40% discrepancies in Ar and 60% in He.

Though an even larger body of charge-transfer data exists (see, e.g., Refs. 1, 4, and 6—12) large areas of ignorance remain. The only CO data is limited to a measurement of σ_{10} over the range 200—1500 keV and there are no measurements of any of the four cross sections for CO_2 below 700 keV. There are large gaps in the N_2 and O_2 data and σ_{12} has been measured for neon only at a single energy.

Most of the previous work has been done over a limited energy range. The present experiment is comprehensive in covering a wide energy range, a large number of targets, and also integrates the various cross-section measurements in a self-consistent manner. This was done by making a least-squares adjustment of the four measured cross sections using the relation

$$\sigma_+ - \sigma_- = \sigma_{10} - \sigma_{12} \,. \tag{1}$$

II. EXPERIMENTAL PROCEDURE

Measurements of the ionization cross sections σ_+ and σ_- were made using the same apparatus and method that was used recently for similar measurements for proton impact,[13] and therefore only a brief description is given here. The electron-transfer cross sections σ_{10} and σ_{12} were measured by a different apparatus which will be described more fully.

A. Accelerators

Four different accelerators at the two laboratories covered overlapping energy ranges. At Pacific Northwest Laboratory (PNL), a low-energy accelerator was used from 10 to 100 keV and a Van de Graaff accelerator from 120 to 2000 keV. The range from 40 to 350 keV was covered by one accelerator at University of Nebraska—Lincoln (UNL) while another UNL accelerator went from 5 to 70 keV. Ionization measurements were made on both PNL accelerators and the higher-energy UNL machine, but electron-transfer cross sections were measured only at the two UNL accelerators. In every case, the beam was magnetically analyzed before reaching the target. The beam energies of the various accelerators used were known to within 0.5% and the energy spread was negligible.

B. Computer interface

A small computer was used with the interface previously described[13] to take the data and calculate cross sections. There were inputs for the pressure, the temperatures of the target and the pressure gauge, and three currents. In

the ionization experiment the currents were the beam current, and the positive and negative currents to the plates. In the electron-transfer measurements the currents were from the three secondary-emission detectors, one for each charge component of the beam after passing through the target. Each current to be measured went to an electrometer, the output of which controlled the frequency of a voltage-controlled oscillator. A scaler in the interface recorded the counts over a 5-sec period, and the count was read by the computer. Since the current-measuring system was calibrated with a picoampere source, and since the output was independent of the meter scale readings, the uncertainty of the current (or accumulated charge) measurements was basically only that of the calibration source, which was 2%.

C. Density determination

Corrections to the readings of the capacitance manometer for the effects of ambient-temperature changes and for thermal transpiration were made as discussed previously.[13] The computer continuously monitored the manometer reading as well as the temperatures of the target-gas cell and the manometer head.

D. Ionization measurement

A transverse field in the target region provided by the collection plates and guard plates served to collect positive ions and electrons from a well-defined beam path length in the target gas. The biases on the plates were chosen to ensure nearly complete collection and had to be adjusted as the energy varied. This was because a compromise had to be made between a field great enough to collect all ejected electrons and yet small enough to avoid deflection of the beam out of the cup. A grid over the ion collection plate suppressed secondary electrons formed at that plate. Corrections for the transmission of the grid and for the secondary electrons formed at the grid were made as described earlier.[13]

Magnetic analysis removed unwanted charge states and impurity ions from the beam but neutralization of the beam after it passed the analyzing magnet had to be considered in the analysis. Measurements of the ionization cross sections at UNL were made at low enough pressures (0.06—0.4 mTorr) that a calculated correction could be made which was less than 5% in all cases, except for neon and helium where at some energies it was as large as 7% and 15%, respectively. At PNL the correction for neutralization was made instead by making measurements at different pressures and extrapolating to zero pressure.

E. Electron-capture and -loss apparatus

Figure 1 shows a schematic diagram of the deflection system used to measure the capture and loss cross sections. The beam passed through an effective length of 9.05 cm of gas in the gas cell (GC). A 6% correction, equal to half the sum of the diameters of the entrance and exit apertures was added to the actual length of the cell to correct for the escape of gas from the cell. The beam then passed between the deflection plates (DP) where the various charge components were separated, each one going to a separate secondary-emission detector (SED). The neutral component of the beam was undeflected and went to the lower detector while the beam components in charge states $+1$ and $+2$ were deflected to the other two detectors.

While the three detectors were identical, the center one was connected as a Faraday cup to read the primary current directly. The other two were used as secondary-emission detectors. The coefficients for the upper and lower cups were measured by deflecting the primary $(1+)$ beam successively into those two detectors and measuring the secondary currents. These currents were compared to the currents read directly when the detectors were connected as Faraday cups. This determination was made at each measured energy since the secondary coefficient varied with impact energy. Because of the different angles of incidence of the beams in the different cups, their coefficients were somewhat different. They varied from 10 to 16 for different energies for the upper cup and from 7 to 13 for the lower cup. We made the assumption that the coefficients did not depend on the charge state of the beam so that we could use the coefficients measured using the $1+$ beam for calculating the neutral and $2+$ beam currents. We checked this assumption for the $2+$ case by measuring the coefficient directly using a beam of that charge state in the upper cup. The secondary coefficient for He^{2+} was found to be about 8% higher than that for He^{+} but since this was well within the 17% uncertainty in the measurement, we decided to use the more accurately measured values for He^{+}. We did not measure the secondary coefficients for He^{0} but other investigators[14] have found only a few percent difference between the coefficients for He^{0} and He^{+} in the present energy range.

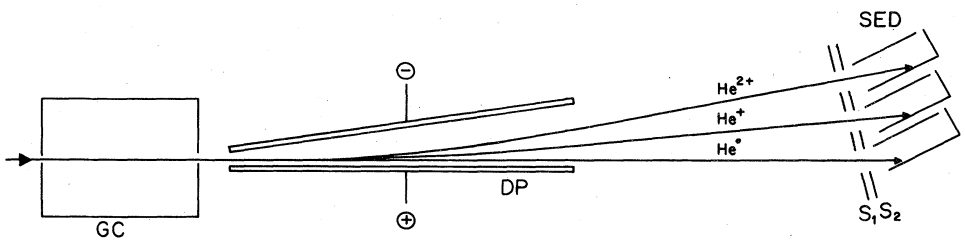

FIG. 1. Apparatus used for measurement of electron-capture and -loss cross sections. Beam passes through gas cell GC. Deflection plates DP deflect the three components of the beam into the secondary-emission detectors SED. Suppressors S_1 and S_2 are to prevent secondary electrons from entering or escaping from the detectors.

F. Data adjustment

If we let σ_{kc} be the cross section for capture of k electrons by the projectile and σ_{jl} be the cross section for the loss of j electrons by the projectile, then by conservation of charge we can write

$$\sigma_+ - \sigma_- = k\sigma_{kc} - j\sigma_{jl} , \tag{2}$$

where σ_+ and σ_- are the cross sections for gross production of positive and negative charge in the target and where the sums are over all possible values of j and k. For a He^+ incident ion, j can only have the value 1, and k the values 1 or 2. Then

$$\sigma_+ - \sigma_- = \sigma_{10} + 2\sigma_{2c} - \sigma_{12} , \tag{3}$$

where we have let σ_{10} stand for σ_{1c}, and σ_{12} stand for σ_{1l}. This result is quite general and holds even if other processes such as dissociation take place. Since σ_{2c}, the cross section for the process in which He^+ becomes He^-, is usually less than 1% of σ_{10}, we can neglect σ_{2c} thus obtaining Eq. (1).

Because of experimental errors, the four measured cross sections do not exactly satisfy Eq. (1). Since the relation is quite rigorously true, a weighted least-squares adjustment of the four cross sections was made to force them to satisfy the equation at each energy. This is a well-known procedure used, e.g., in adjusting interrelated values of fundamental constants. Weights for each type of cross section at each energy were chosen to be inversely proportional to the estimated fractional systematic error in the measurements. This error was taken to be of the form $F = A + B/E$ where E was the energy in keV. The values of A were taken to be 0.1, 0.1, 0.1, and 0.15 and the values of B to be 5, 0.3, 0.15, and 1.5 for σ_+, σ_-, σ_{10}, and σ_{12}, respectively. The error was larger at the low energies primarily because of difficulties in controlling the beam. Using the method of Lagrange multipliers, an algorithm was derived which minimized the fractional adjustments.

The final data reported here reflect the results of this adjustment up to 350 keV which is the highest energy for which we took electron-transfer data. Above that point the ionization data did not benefit from this adjustment, but in all cases the adjustments near 350 keV were less than 3%. In fact, the adjustments never exceeded the quoted uncertainties in the cross sections at any energy. This adjustment procedure gives the data an internal consistency which it would not otherwise have.

G. Uncertainties

In the following analysis of uncertainties, the generally small variations among the various target gases have been disregarded. The determination of density in all measurements was uncertain by 4%. For σ_+ and σ_- the uncertainty in the collection of the beam varied from 12% at 10 keV to 3% at 100 keV and above. The correction for background currents to the collecting plates went from 10% at 10 keV to a negligible value at 100 keV. For unknown reasons, the day-to-day fluctuations of the current to the ion collecting plate were as large as 50% at the lowest energies. This uncertainty decreased to 10% at 100 keV. The fluctuations for σ_- were 8—10%.

For the electron-transfer measurements, the effective length of the beam in the target gas was uncertain by 7%. A 7% uncertainty was assigned to the secondary-emission coefficient for He^0 and 12% for He^{2+}. Since the pressure in the chamber was typically a factor of 50—100 times smaller than that in the target-gas cell, the change in charge of the separated beam before the detectors was less than 1% even in the worst case. In the measurement of σ_{12} the small size of the currents caused an additional uncertainty which was typically 50% at the lowest energies (10—20 keV usually) dropping to 5% above 50 keV. In the larger currents obtained in the σ_{10} measurements the uncertainties were only about 2%.

The average deviations of the cross sections from the smoothed curves were 6% for σ_+, 4% for σ_-, 6% for σ_{10}, and 11% for σ_{12}, although as noted above, the fluctuations were larger for σ_+ at the lowest energies. The algorithm given above may be used to calculate the uncertainties at various energies for the different cross sections.

H. Experimental results

In Figs. 2 and 3 are shown sample data taken with the various accelerators after correction for beam neutralization. While in some cases there were disagreements among the overlapping data sets, generally the agreement was good. Smooth curves were drawn through the average of the data and values read from these curves were used in the least-squares adjustment.

Tables I—IV give the final adjusted values of the four cross sections and Figs. 4—6 show a comparison of our values, shown as lines, with the data of various other investigators.

1. Helium

The largest discrepancy between the present data and that of earlier investigators occurs for helium. In our earlier proton work[13] the σ_- data for helium was significantly lower at the lowest energies than earlier data. The same is true to an even greater extent in the present case where the discrepancy which starts at about 60 keV grows

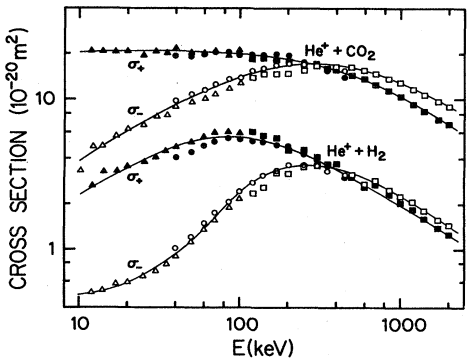

FIG. 2. Unadjusted values of σ_+ (solid symbols) and σ_- (open symbols) for He^+ on CO_2 and H_2. Triangles and squares are PNL data, circles UNL data. Solid lines represent the smoothed data.

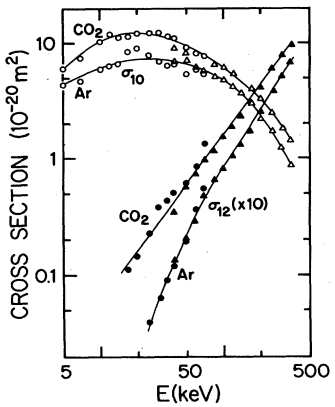

FIG. 3. Unadjusted values of σ_{10} (open symbols) and σ_{12} (solid symbols) for He^+ on CO_2 and Ar. Triangles are high-energy UNL accelerator data and circles are from the low-energy UNL accelerator. Solid lines represent the smoothed data.

to a factor greater than 5 at 10 keV as seen in Fig. 4. Because of the small size of the helium cross sections, they are especially vulnerable to problems of target contamination and spurious electrons, both of which result in measured cross sections which are too large. We believe that these effects could explain the discrepancy here as in the proton case. Supporting our data is the fact that the general shape of our He cross-section curve is similar to that for other gases, while the leveling off of the curve at low energies seen, e.g., in DeHeer's data,[4] is not characteristic. There is generally good agreement with the data of Pivovar *et al.*[5] at high energies and with Langley *et al.*[2] above 400 keV.

Our σ_+ data was found to be in good agreement with that of Langley *et al.*,[2] DeHeer *et al.*,[4] Solov'ev *et al.*,[3] and Pivovar *et al.*[5] Our σ_{10} data agrees well with that of DeHeer *et al.*,[4] but is 12—20% higher than that of Pivovar *et al.*[5] at high energies. The σ_{12} data agrees well with that of Shah *et al.*,[10] but is 12—50% higher than that of Pivovar *et al.*[8] as seen in Fig. 6.

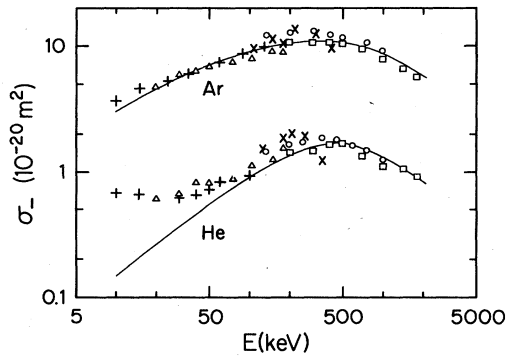

FIG. 4. Comparison of present σ_- data, represented by the line, and data of other investigators for He^+ on He and Ar. Pivovar *et al.* (Ref. 5), □; Solov'ev *et al.* (Ref. 3), △; Langley *et al.* (Ref. 2), ○; Gilbody *et al.* (Ref. 1), ×; DeHeer *et al.* (Ref. 4), +.

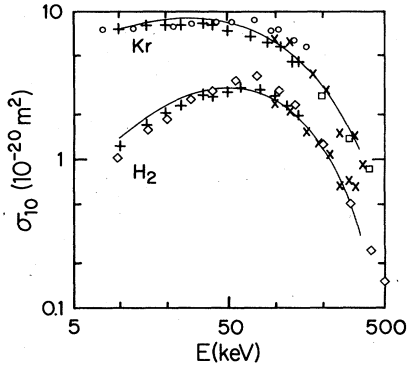

FIG. 5. Comparison of present σ_{10} data, represented by the line, and data of other investigators for Kr and H_2. Pivovar *et al.* (Ref. 8), □; DeHeer *et al.* (Ref. 4), +; Olson *et al.* (Ref. 9), ◇; Fedorenko *et al.* (Ref. 7), ○; Gilbody *et al.* (Ref. 1), ×.

2. Neon

Our σ_+ and σ_- data are in very good agreement with that of DeHeer *et al.*[4] and with other earlier measurements. The only exception is that at about 130 keV there is a discrepancy between DeHeer *et al.*[4] and Langley *et al.*,[2] and our data favor the former. Our σ_{10} cross sections are uniformly 20—25% higher than those of Gilbody *et al.*[1] but are in good agreement with the average of all the other measurements. The only previous neon σ_{12} data were by Jones, *et al.*[6] with which we are in good agreement as shown in Fig. 6.

3. Argon

Our σ_+ and σ_- data are in generally good agreement with earlier data except for that of Langley *et al.*[2] which is 10—35% higher. No serious disagreements exist in the σ_{10} or σ_{12} data compared to earlier data.

4. Krypton

Our results are in good agreement with the data of DeHeer *et al.*[4] and Pivovar *et al.*[5] for both σ_+ and σ_-.

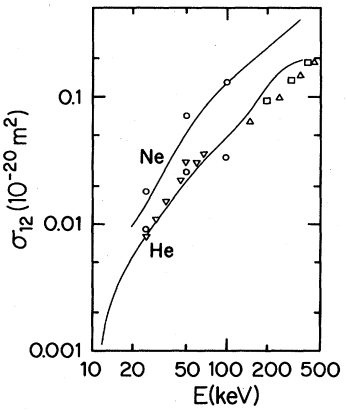

FIG. 6. Comparison of present σ_{12} data, represented by the line, with data of other investigators. Jones *et al.* (Ref. 6), ○; Allison (Ref. 12), △; Shah and Gilbody (Ref. 10), ▽; Pivovar *et al.* (Ref. 8), □.

TABLE I. Values of σ_+ for He^+ collisions. Units are 10^{-20} m^2.

Energy (keV)	He	Ne	Ar	Kr	H_2	N_2	CO	O_2	CH_4	CO_2	Fract. Unc.
10	6.2	8.4	9.5	12	2.0	11	13	12	12	15	0.60
14	5.8	8.4	11	13	2.4	12	13	13	13	17	0.46
20	5.3	7.8	12	14	3.0	13	14	13	14	19	0.35
30	4.7	7.0	13	16	3.6	14	14	14	14	20	0.27
40	4.1	6.3	14	16	4.1	14	14	14	14	20	0.23
60	3.6	5.7	14	17	4.6	14	14	13	15	20	0.18
85	3.2	5.4	14	16	4.9	14	14	13	15	20	0.16
120	2.9	5.1	13	16	5.0	13	13	12	14	20	0.14
170	2.6	4.9	12	15	4.9	13	13	12	14	19	0.13
250	2.2	4.6	12	14	4.3	12	12	11	13	18	0.12
350	1.9	4.3	10	14	3.6	11	11	10	12	17	0.11
500	1.7	4.0	9.4	12	3.0	9.3	9.6	9.0	11	14	0.11
700	1.4	3.5	8.0	11	2.4	7.8	8.3	8.0	9.8	12	0.11
1000	1.1	3.0	6.5	9.2	2.0	6.5	6.9	6.8	8.0	10	0.11
1400	0.88	2.4	5.3	7.7	1.6	5.4	5.6	5.8	6.5	8.5	0.10
2000	0.68	1.9	4.2	6.1	1.2	4.3	4.5	4.8	5.0	6.6	0.10

TABLE II. Values of σ_- for He^+ collisions. Units are 10^{-20} m^2.

Energy (keV)	He	Ne	Ar	Kr	H_2	N_2	CO	O_2	CH_4	CO_2	Fract. Unc.
10	0.14	0.84	3.0	4.3	0.52	3.9	4.4	2.9	3.9	4.1	0.13
14	0.20	0.90	3.7	5.1	0.54	4.5	4.6	3.4	4.5	5.1	0.12
20	0.26	1.0	4.6	5.9	0.61	5.1	5.1	4.1	5.2	6.3	0.12
30	0.36	1.4	5.6	6.8	0.77	5.8	5.9	5.0	6.0	8.0	0.11
40	0.46	1.7	6.5	7.6	0.98	6.5	6.4	5.7	6.8	9.4	0.11
60	0.62	2.2	7.6	8.7	1.5	7.4	7.6	6.9	7.9	11	0.11
85	0.80	2.6	8.5	9.7	2.1	8.2	8.4	7.8	8.7	13	0.10
120	0.99	3.0	9.2	11	2.8	9.2	9.1	8.8	9.7	14	0.10
170	1.2	3.4	9.9	12	3.4	9.9	9.9	9.4	11	16	0.10
250	1.5	3.8	10	12	3.6	10	10	9.9	12	16	0.10
350	1.7	4.0	10	13	3.5	10	11	9.9	12	16	0.10
500	1.7	4.1	10	13	3.2	10	11	9.6	12	16	0.10
700	1.5	4.0	9.7	12	2.8	9.4	9.7	9.1	12	15	0.10
1000	1.3	3.6	8.6	11	2.2	8.2	8.5	8.4	9.2	13	0.10
1400	1.1	3.1	7.2	9.9	1.8	7.0	7.3	7.3	7.5	11	0.10
2000	0.83	2.6	5.7	8.2	1.4	5.7	6.0	6.2	6.0	8.8	0.10

TABLE III. Values of σ_{10} for He^+ collisions. Units are 10^{-20} m^2.

Energy (keV)	He	Ne	Ar	Kr	H_2	N_2	CO	O_2	CH_4	CO_2	Fract. Unc.
5	6.0	6.1	4.8	6.0	0.64	3.4	5.7	8.0	8.1	6.2	0.13
7	6.3	7.0	5.7	6.8	0.96	5.3	7.1	8.8	8.3	8.6	0.12
10	6.1	7.6	6.5	7.5	1.4	6.7	8.4	9.2	8.4	11	0.12
14	5.6	7.5	7.1	8.2	1.9	7.7	8.9	9.5	8.4	12	0.11
20	5.1	6.8	7.4	8.6	2.4	8.2	8.8	9.4	8.4	12	0.11
30	4.3	5.6	7.4	8.9	2.8	8.0	8.4	8.6	8.2	12	0.11
40	3.7	4.6	7.1	8.7	3.1	7.6	7.7	7.8	7.8	11	0.10
60	3.0	3.6	6.2	8.0	3.1	6.6	6.6	6.4	6.9	8.7	0.10
85	2.5	2.8	5.3	6.9	2.8	5.6	5.4	5.2	6.0	7.0	0.10
120	2.0	2.2	4.1	5.4	2.2	4.4	4.3	4.0	4.7	5.3	0.10
170	1.4	1.6	2.9	3.9	1.5	3.1	3.0	2.8	3.4	3.9	0.10
250	0.85	1.1	1.7	2.2	0.78	1.8	1.8	1.7	2.0	2.5	0.10
350	0.45	0.71	0.87	1.1	0.30	0.95	0.94	0.98	1.0	1.4	0.10

TABLE IV. Values of σ_{12} for He^+ collisions. Units are 10^{-20} m^2.

Energy (keV)	He	Ne	Ar	Kr	H_2	N_2	CO	O_2	CH_4	CO_2	Fract. Unc.
7							0.0019				0.36
10						0.0036	0.0034	0.0050			0.30
14	0.0026					0.0058	0.0058	0.0085	0.0020	0.0091	0.26
20	0.0056	0.010			0.0013	0.010	0.010	0.015	0.0040	0.015	0.23
30	0.011	0.021	0.0055	0.0013	0.0022	0.017	0.018	0.028	0.0086	0.028	0.20
40	0.016	0.036	0.012	0.0028	0.0033	0.027	0.028	0.043	0.015	0.043	0.19
60	0.028	0.068	0.031	0.0086	0.0061	0.049	0.053	0.077	0.031	0.078	0.18
85	0.041	0.11	0.065	0.022	0.012	0.086	0.088	0.13	0.057	0.13	0.17
120	0.059	0.15	0.12	0.050	0.024	0.15	0.15	0.21	0.10	0.22	0.16
170	0.095	0.20	0.20	0.11	0.067	0.29	0.25	0.32	0.17	0.36	0.16
250	0.16	0.29	0.41	0.23	0.13	0.53	0.45	0.52	0.32	0.63	0.16
350	0.20	0.40	0.70	0.43	0.17	0.82	0.76	0.79	0.52	1.0	0.15

Our σ_{10} data, shown in Fig. 5, agree well with that of DeHeer *et al.*,[4] and with that of Gilbody *et al.*,[1] but are generally lower than those of Fedorenko *et al.*[7] There is no previous σ_{12} data below 200 keV but above that energy we agree well with Pivovar *et al.*[8]

5. *Hydrogen*

The present ionization data agree well with most of the earlier work except that it is somewhat higher in the 500—1500-keV range especially when compared with the data of Langley *et al.*[2] The σ_{10} data, shown in Fig. 5, are generally between those of Olson *et al.*,[9] and those of Gilbody *et al.*,[1] except below 40 keV where our cross sections are higher than the earlier measurements. Our measurements of σ_{12} agree well with those of Barnett *et al.*[11]

6. *Nitrogen*

The present σ_- data agree well with those of Solov'ev *et al.*,[3] and Pivovar *et al.*,[8] but are lower than those of Langley *et al.*,[2] and DeHeer *et al.*[4] Langley's σ_+ data are also higher than ours.

7. *Carbon monoxide*

The only data previously available are by Langley *et al.*[2] for σ_+ and σ_- of 133—1000 keV. Our data agrees with theirs within 5—10% at the upper end of their energy range, but are as much as 45% lower at 133 keV. No data on σ_{12} or σ_{10} are known for carbon monoxide in this energy range.

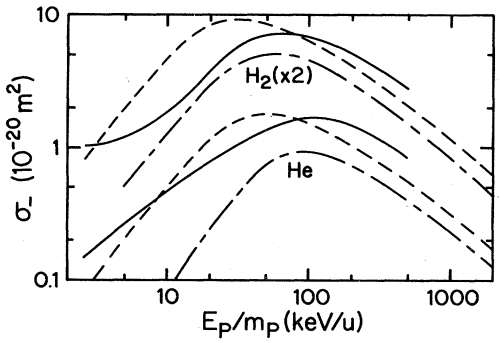

FIG. 7. Comparison of ionization of H_2 and He by He^+, solid line; and by H^+, dash-dot line. The energy scale of the proton data is adjusted to compare equal velocity projectiles. Theoretical calculations by Boyd *et al.* (Ref. 13) are shown as the dashed line.

8. *Carbon dioxide, methane*

To our knowledge, no data for any of the four cross sections have been published for either of these gases in the present energy range.

I. Comparison with theory

Little theoretical attention has been paid to ionization by helium ions. Boyd *et al.*[15] have calculated cross sections for He^+ on hydrogen atoms using the Born approximation. They present calculations for ionization of the H atom and also for electron loss from the He^+ projectile in which the H atom is left in the ground states, various excited states, or the continuum. Recently Manson and Toburen[16] have presented cross sections for the energy and angular distributions of electrons ejected in $He^+ + He$ collisions but only at 2 MeV. This calculation also includes projectile ionization as well as target ionization but no total ionization cross sections were given.

In Fig. 7 the present results for ionization of H_2 and He are shown along with the calculations of Boyd *et al.*[15] These were scaled according to the equation

$$\sigma_-(E_P,B,N)=N(R/B)^2\sigma_-(E_PB/R,R,1)$$

where B is the binding energy, N the number of electrons in the target atom, E_P is the projectile energy, and R is 13.6 eV. For this scaling, we have taken B to be 24.6 eV and 15.4 eV for helium and hydrogen, respectively. We have added the contributions calculated by Boyd for ionization of the target and the sum of the projectile ionizations with various excitations. As expected, target ionization provides most of the contribution. While the general shapes of the theoretical curves are similar to our experimental He^+ curves, the maxima come at different energies and the general agreement is not good.

Also shown in Fig. 7 are the cross sections for ionization by protons. One notes a similarity in shape but that

He^+ produces somewhat larger ionization cross sections. Manson and Toburen[16] argue that the He^+ projectile acts like a proton for small electron ejection energies but like a He^{2+} ion for large energy transfers to the electron. Since the average ejection energy increases with increasing projectile energy up to about 300 keV for protons,[17] and since the cross sections should scale approximately as Z_P^2, there should therefore, be an increasing spread between the cross sections for He^+ and those for H^+ as the energy is increased. Our data indeed shows this expected behavior for energies above the maximum. Below the maximum the ionization is expected to proceed more by the molecular promotion mechanism, for which a different analysis must be used.

ACKNOWLEDGMENTS

This paper is based on work performed under National Science Foundation Grant No. PHY-82-43326 and the U.S. Department of Energy Contract No. DE-AC06-76RL01830. We wish to thank Robert Bass and David Fox for assistance in taking the data at the University of Nebraska—Lincoln.

*Present address: 3 Eglantine Park, Hillsborough, County Down BT26 6HL, North Ireland.

[1]H. B. Gilbody, J. B. Hasted, J. V. Ireland, A. R. Lee, E. W. Thomas, and A. S. Whiteman, Proc. Phys. Soc. London **274**, 40 (1963).

[2]R. A. Langley, D. W. Martin, D. S. Harmer, J. W. Hooper, and E. W. McDaniel, Phys. Rev. **136**, A379 (1964).

[3]E. S. Solov'ev R. N. Il'in, V. A. Oparin, and N. V. Fedorenko, Zh. Eksp. Teor. Fiz. **45**, 496 (1963) [Sov. Phys.—JETP **18**, 342 (1964)].

[4]F. J. DeHeer, J. Schutten, and H. Moustafa, Physica (Utrecht) **32**, 1793 (1966).

[5]L. I. Pivovar, Yu. Z. Levchenko, and A. N. Grigor'ev, Zh. Eksp. Teor. Fiz. **54**, 1310 (1967) [Sov. Phys.—JETP **27**, 699 (1968)].

[6]P. R. Jones, F. P. Ziemba, H. A. Moses, and E. Everhart, Phys. Rev. **113**, 182 (1959).

[7]N. V. Fedorenko, V. V. Afrosimov, and D. M. Kaminker, Sov. Phys. Tech. Phys. **1**, 1861 (1956).

[8]L. I. Pivovar, V. M. Tubaev, and M. T. Novikov, Zh. Eksp. Teor. Fiz. **41**, 26 (1961) [Sov. Phys.—JETP **14**, 20 (1962)].

[9]R. E. Olson, A. Salop, R. A. Phaneuf, and F. W. Meyer, Phys. Rev. A **16**, 1867 (1977).

[10]M. B. Shah and H. B. Gilbody, J. Phys. B **8**, 372 (1975).

[11]C. F. Barnett and P. M. Stier, Phys. Rev. **109**, 385 (1958).

[12]Samuel K. Allison, Rev. Mod. Phys. **30**, 1137 (1958).

[13]M. E. Rudd, R. D. DuBois, L. H. Toburen, C. A. Ratcliffe, and T. V. Goffe, Phys. Rev. A **28**, 3244 (1983).

[14]P. M. Stier, C. F. Barnett, and G. E. Evans, Phys. Rev. **96**, 973 (1954).

[15]T. J. M. Boyd, B. L. Moisewitsch, and A. L. Stewart, Proc. Phys. Soc. London, Sect. A **70**, 110 (1957).

[16]Steven T. Manson and L. H. Toburen, Phys. Rev. Lett. **46**, 529 (1981).

[17]M. E. Rudd, L. H. Toburen, and N. Stolterfoht, At. Data Nucl. Data Tables **23**, 405 (1979).